Materials Chemistry and Physics 134 (2012) 958–965

Contents lists available at SciVerse ScienceDirect

Materials Chemistry and Physics

journal homepage: www.elsevier.com/locate/matchemphys

Prescribed morphology and interface correlation of MWNTs-EP/PSF hybrid nanofibers reinforced and toughened epoxy matrix

Gang Li [a,b,*], Xiaolong Jia [b], Zhibin Huang [b], Bo Zhu [b], Peng Li [b], Xiaoping Yang [b,*], Wuguo Dai [c]

[a] College of Mechanical and Electrical Engineering, Beijing University of Chemical Technology, Beijing 100029, PR China
[b] State Key Laboratory of Organic–Inorganic Composites, Beijing University of Chemical Technology, Beijing 100029, PR China
[c] Nantong XingChen Synthetic Materials Co., China BlueStar Co., Nantong 226017, PR China

ARTICLE INFO

Article history:
Received 21 May 2011
Received in revised form
30 January 2012
Accepted 23 March 2012

Keywords:
Interfaces
Nanostructures
Electron microscopy
Fracture and toughness

ABSTRACT

MWNTs-EP were successfully prepared by functionalization of MWNTs with epoxy-based groups, and MWNTs-EP/polysulfone (PSF) hybrid nanofibers were fabricated to obtain ex-situ dispersion and alignment of MWNTs-EP by electrospinning. The prescribed morphology and interface correlation of hybrid nanofibers reinforced and toughened epoxy matrix (RTEP) were investigated. The alignment degree of hybrid nanofibers was enhanced with increasing MWNTs-EP loadings, and MWNTs-EP were found to be well dispersed and aligned along the nanofiber axis. The dispersion and alignment states of MWNTs-EP during inhomogeneous phase separation of RTEP were proposed and verified. MWNTs-EP dispersed and aligned along the orginal nanofiber axis were enveloped, bridged or pinned by PSF spheres arranged in the nanofiber direction. The interface chemical correlation between MWNTs-EP and resin matrix was generated due to the further reaction of epoxide rings on the surface of MWNTs-EP, which resulted in simultaneous improvement of mechanical and thermal properties of RTEP.

1. Introduction

Since carbon nanotubes (CNTs) were first used as filler in epoxy matrix in the mid 1990s, CNT reinforced epoxy matrix have been explored as new prospects for superior composite materials with high strength, low weight and multi-functional features [1–3]. However, the atomically smooth nonreactive surfaces, the distinctively poor interfacial bonding, and the spontaneously entangled aggregation properties have limited the effectiveness of CNTs [4,5]. Therefore, the strong interfacial interaction between CNTs and matrix as well as the homogenous dispersion of CNTs in the epoxy matrix should be a pre-requisite in order to obtain high performance polymer composites [6,7]. For this purpose, chemical functionalization of the surface of CNTs has been proposed as an efficient method [8–10] to improve the interfacial stress transfer and positively affect the dispersibility of CNTs. Epoxy-based functionalization of CNTs was shown to be the most favorable due to the ability of further reacting of epoxide groups grafted on the surface of CNTs [11].

Another important aspect to be considered for these materials was the nano- and micro- morphology of reinforcement phase and reinforced composites [2,12]. Vaia [13] has suggested the idea of "nanocomposites-by-design", and tried to establish structure-performance correlations of composites by controlling the distribution and arrangement of dispersed, preformed CNTs. Xie [14] and Esawi [15] also considered that the enhanced dispersion and alignment of CNTs in the polymer matrix were directly related to the mechanical and functional properties of CNTs/polymer composites. To optimize the properties of CNTs/polymer composites, Raravikar [16] and Feng [17] pointed out that the dispersion and alignment of CNTs could be achieved prior to composite fabrication where aligned nanotubes are incorporated into the polymer matrix using an external electric field. Therefore, various processing techniques have been exploited to establish the coupling between applied external forces and the distribution and alignment of CNTs [18–20]. At present, fiber spinning is considered as effective method to possess the ability to induce ex-situ dispersion and alignment of CNTs by mechanical deformation. The electrospinning process has been successfully used to disperse and align CNTs in polymer composite nanofibers, in which the stable dispersion and high alignment of CNTs were obtained [21,22].

In our previous work, the inhomogeneous phase structures have been observed in polysulfone (PSF) nanofibers toughened epoxy

* Corresponding authors. State Key Laboratory of Organic–Inorganic Composites, Beijing University of Chemical Technology, Beijing 100029, PR China. Tel./fax: +86 1064412084.
E-mail addresses: ligang@mail.buct.edu.cn (G. Li), yangxp@mail.buct.edu.cn (X. Yang).

0254-0584/$ – see front matter © 2012 Elsevier Ltd. All rights reserved.
doi:10.1016/j.matchemphys.2012.03.098

matrix [23,24], and PSF spheres generated from phase separation of nanofibers exhibited random alignment. On the basis of the inhomogeneous phase separation, the electrospinning-induced dispersion and alignment of CNTs were introduced to fabricate CNTs/PSF hybrid nanofibers with well dispersed and aligned CNTs, and to prepare reinforced and toughened epoxy matrix (RTEP) using such hybrid nanofibers. During the inhomogenenous phase separation of hybrid nanofibers, the CNTs were well dispersed and aligned in the phase structure due to the ex-situ dispersion and alignment of CNTs in hybrid nanofibers. Therefore, the prescribed morphology of RTEP was obtained that could achieve the synergistic effects of the improvement of strength and toughness.

To achieve this purpose, (i) MWNTs-EP were prepared by carboxylation and further attachment of epoxy terminated molecules, and MWNTs-EP/PSF hybrid nanofibers with well dispersed and highly aligned MWNTs-EP were fabricated by electrospinning, (ii) a schematic representation of the dispersion and alignment state of MWNTs-EP during the inhomogeneous phase separation of hybrid nanofibers was proposed, and compared with the actual morphologies of RTEP, (iii) the chemical correlation between MWNTs-EP and epoxy matrix interfaces were investigated, and the mechanical and thermal properties of RTEP were also discussed.

2. Experimental

2.1. Materials

Multiwalled carbon nanotubes (MWNTs, purity≥95%, diameter 10–20 nm, length 5–15 μm) were produced by Shenzhen Nanotech Port Co., Ltd, China. Polysulfone (PSF, Udel 1700) was supplied by Amoco Co. Diglycidol ether of bisphenol A (DGEBA, EPON 828) was obtained from Shell Chemical Co. 4,4′-diaminodiphenylsulfone (DDS) were manufactured by Yinsheng Chemical Co. N,N′-dimethyl formamide (DMF), triphenyl phosphorus (TPP), tetrahydrofuran (THF), N,N′-dimethyl acetamide (DMAC) and acetone were purchased from Beijing Chemical Agent Co.

2.2. Preparation of MWNTs-EP

The schematic of the preparation procedure for epoxy grafted MWNTs (MWNTs-EP) is shown in Fig. 1. The carboxylated MWNTs was prepared by following our previously reported procedure [21]. The carboxyl groups were first introduced onto the surface of the MWNTs by acid oxidation of as-received MWNTs for 1 h with a mixture of concentrated H_2SO_4 and HNO_3 (1:1, volume ratio). The carboxylated MWNTs were dispersed in DMF by bath sonication for 1 h. DGEBA was dissolved in DMF in a separate vessel, after which the two dissolved materials were further mixed and bath-sonicated for half an hour. Then the mixture was slowly stirred and heated to 130 °C, after adding TPP as a catalyst for the reaction. The system was allowed to react for 12 h. The reacted MWNTs were washed with THF and filtered through a PTFE with a 2 μm pore size to obtain the epoxy grafted MWNTs (MWNTs-EP).

2.3. Fabrication of MWNTs-EP/PSF hybrid nanofibers

MWNTs-EP were dispersed in 20 ml mixture of DMAC/acetone (7:3 volume ratio) by ultrasonic agitation for 6 h, then 4.0 g PSF pellets were added to obtain a suspension for electrospinning. The suspension was placed in 30 ml medical syringe with 12 gauge needle, and electrospun at 0.5 ml/h flow rate under 16 kV applied voltage. The amount of MWNTs-EP in hybrid nanofibers was controlled to 5, 10, 15 wt % of PSF. For comparison, PSF nanofibers without MWNTs-EP were prepared by electrospinning.

2.4. Preparation of hybrid nanofibers reinforced and toughened epoxy (RTEP)

Epoxy matrix was prepared by dissolving 100 g of DGEBA and 30 g of DDS by vigorous stirring at 120 °C for 25 min, and the blend was degassed under vacuum to obtain homogeneous solution. PSF nanofibers and hybrid nanofibers with various MWNTs-EP loadings were cut and placed horizontally into a laboratory-made mold. The epoxy matrix was then poured into the mold and cured at three stages: 120 °C for 2 h, 160 °C for 2 h, and 180 °C for 1 h. The amount of the nanofibers was controlled to 2 wt % of resin matrix, that is, the MWNTs-EP loadings were controlled to 0.1, 0.2 and 0.3 wt % in RTEP, respectively.

2.5. Characterization

Changes of the functional groups on the surface of MWNTs were detected with an FTIR spectrometer (Nicolet 670).

Morphologies of PSF nanofibers, MWNTs-EP/PSF hybrid nanofibers and the nanofibers reinforced and toughened epoxy matrix, were observed by scanning electron microscope (SEM, S 4700, HITACHI) and transmission electron microscope (TEM, JEM100CX, HITACHI), respectively.

The alignment of MWNTs-EP in the hybrid nanofibers was characterized using Raman spectrometer (TY-HR 800) with laser excitation at 532 nm.

The tensile properties were measured by tensile testing machine (INSTRON 1121) according to GB 2568-1995. The dumbbell specimens of dimension 100 mm × 6 mm × 2.5 mm was prepared by the nanofiber direction parallel to the length of specimens, and tested at a rate of 1 mm/min using a 5 kN load cell. The final values were averages of five measurements.

Dynamic mechanical thermal analysis was performed by three-point bending mode (DMTA-V, Rheometrics Scientific Co. USA). The dimension of a specimen for DMTA testing was 50 mm × 6 mm × 2 mm. The heating rate was 5 °C/min from 50 °C to 300 °C, and the fixed frequency was 1 Hz. The T_g was measured from the peak of the tan δ spectrum.

The critical stress intensity factor (K_{IC}) was measured by single-edge notched fracture toughness test in three-point bending mode, according to ASTM 5045-1999. The crosshead rate was 1 mm/min, and the final values were averages of five measurements.

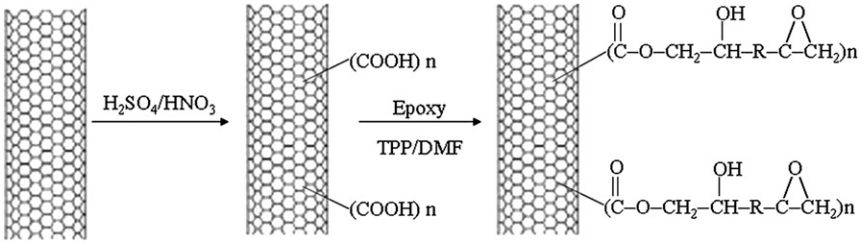

Fig. 1. Schematic of the preparation procedure for MWNTs-EP.

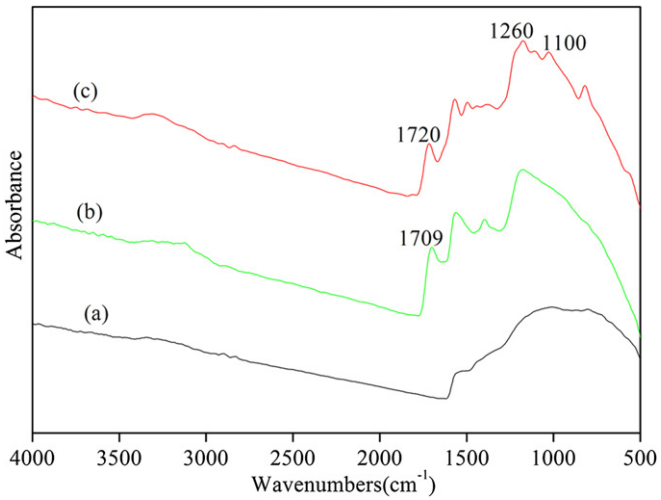

Fig. 2. FTIR spectra of (a) as-received MWNTs, (b) carboxylated MWNTs, and (c) MWNTs-EP.

3. Results and discussion

3.1. Functionalization of MWNTs

Fig. 2 shows the FTIR spectra of as-received MWNTs, carboxylated MWNTs and MWNTs-EP. The peak at 1709 cm^{-1} in the spectra of carboxylated MWNTs corresponded to the carboxyl of the carboxylic acid, which indicated the changes of functional groups on the surface of MWNTs due to the carboxylation [5]. This peak was not detected on the as-received MWNTs. In the spectra of MWNTs-EP, the disappearance of the peak at 915 cm^{-1}, which corresponded to the epoxide ring in the DGEBA [5], indicated that the epoxide rings opened and reacted. The peak at 1100 cm^{-1} was related to the C—O bond which resulted from the reaction between the carboxylic acid and the epoxide ring. The peak at 1260 cm^{-1} was associated with C—O of the ester, which was attached to the aromatic rings of MWNTs [11], as shown in Fig. 1. These results indicated that the epoxide-terminated groups were successfully grafted onto the surface of MWNTs.

3.2. Morphology of MWNTs-EP/PSF hybrid nanofibers

Fig. 3 shows the SEM images of MWNTs-EP/PSF hybrid nanofibers with 0, 5, 10, and 15 wt % MWNTs-EP. PSF nanofiber without MWNTs-EP possessed coarser diameter with more random distribution than hybrid nanofibers with MWNTs-EP. With increasing MWNTs-EP loadings, the average diameter of nanofibers decreased along with the enhancement of alignment degree, as shown in Fig. 3b–d. In general, the electric conductivity of MWNT-EP/PSF suspensions for electrospinning increased with increasing MWNTs-EP loadings, which led to the increase of net charge density carried by the spinning jet [25]. Therefore, the liquid droplet of the suspensions were subjected to the larger electrostatic forces, and the spinning jet underwent the larger draw ratios during the electrospinning process [26], which allowed the dissolved polymer to be oriented by the elongational flow of the charged jet [25], finally resulting in the increase of the degree of alignment of hybrid nanofibers.

Fig. 4 shows the TEM images of MWNT-EP/PSF hybrid nanofibers with 5, 10, and 15 wt% MWNTs-EP. The MWNTs-EP were successfully embedded in the PSF nanofibers, and were well dispersed and highly aligned along the nanofiber axis. The degree of alignment of MWNTs-EP increased with increasing MWNTs-EP loadings. When the loading of MWNTs-EP in the nanofiber was reached 15 wt %, the MWNTs-EP were almost stretched into stream lines, which was attributed to the extremely large effective draw ratio resulted from bending instability in the electrospinning process [20]. The increase of the degree of alignment of MWNTs-EP in hybrid nanofibers might be favorable to the dispersion and orientation of MWNTs-EP in epoxy matrix.

The alignment of MWNTs-EP in hybrid nanofibers was further characterized with Raman Spectroscopy. Fig. 5 shows the polarized Raman spectra of MWNTs-EP/PSF hybrid nanofibers with 5, 10, and 15 wt % MWNTs-EP, in which the VV curve represented the

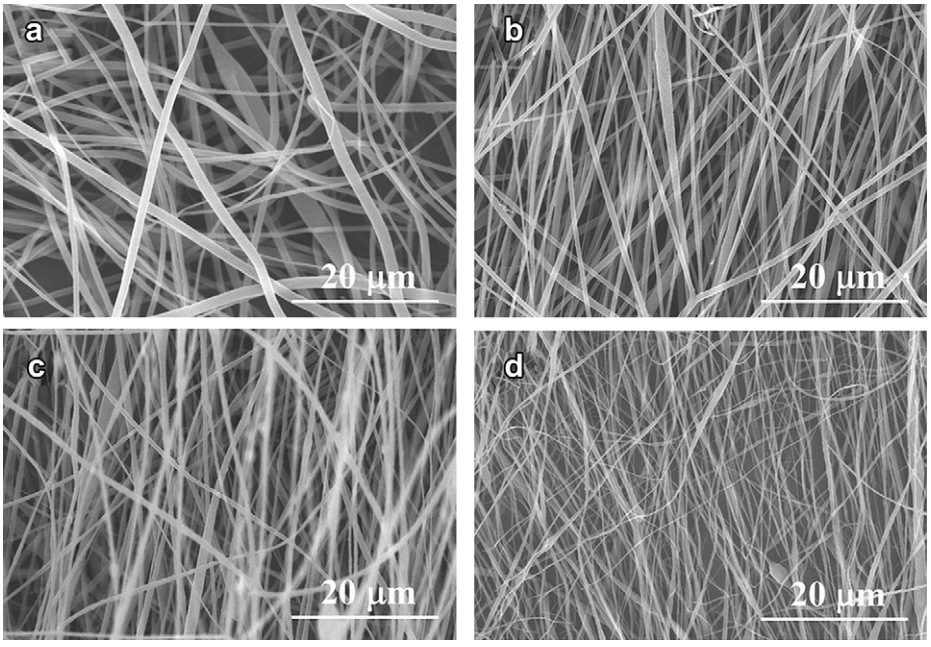

Fig. 3. SEM images of MWNTs-EP/PSF hybrid nanofibers with (a) 0, (b) 5, (c) 10, and (d) 15 wt % MWNTs-EP.

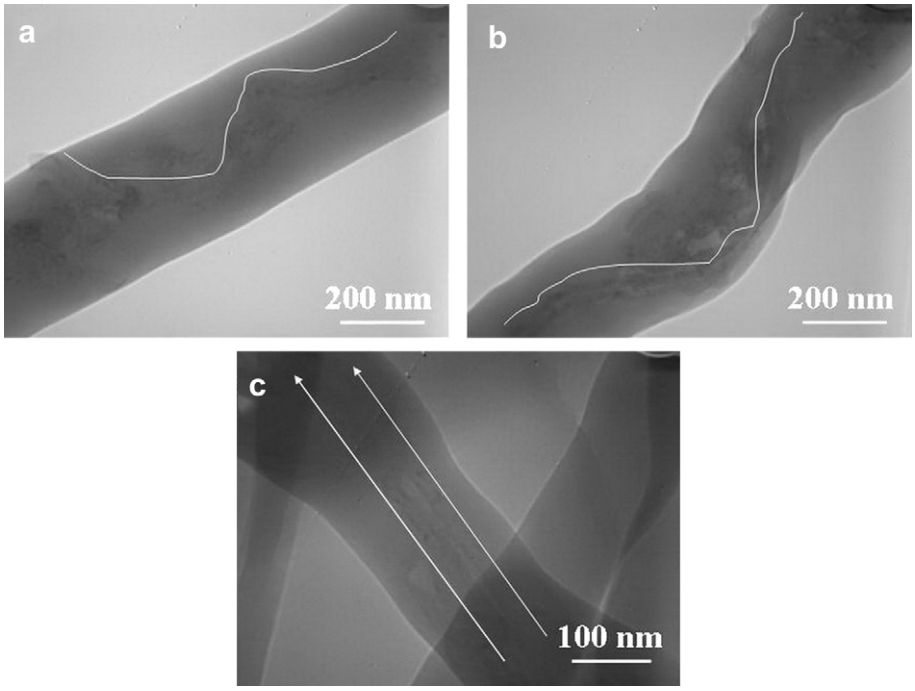

Fig. 4. TEM images of MWNTs-EP/PSF hybrid nanofibers with (a) 5, (b) 10, and (c) 15 wt % MWNTs-EP. (The white curves in part a and b and the white arrows in part c represent the alignment directions of the MWNTs-EP.)

spectrum when the polarization of the incident laser was parallel to the nanofiber axis, and the VH curve represented the spectrum when the polarization of the incident laser was normal to the nanofiber axis. The strong absorption peak at 1582 cm^{-1} was assigned as the G band and associated with tangential C–C bond stretching motion that originated from the E_{2g2} mode in the graphite. The peak at 1351 cm^{-1} was assigned as the D band and derived from disordered graphite structures [27]. The shoulder peak at 1607 cm^{-1} was usually denoted as the D′ band and has also been attributed to disorder-induced features in the CNTs [28]. With increasing MWNTs-EP loadings, the up-shift of G and D bands indicated that MWNTs-EP possessed a substantial interaction [27], which might be attributed to better compatibility between PSF and epoxy on the surface of MWNTs-EP. In addition, there was an obvious difference in the intensity of the G band for different polarization directions with increasing MWNTs-EP loadings, which was associated with the alignment of CNTs in the hybrid nanofibers. In general, the degree of alignment of CNTs can be evaluated by the

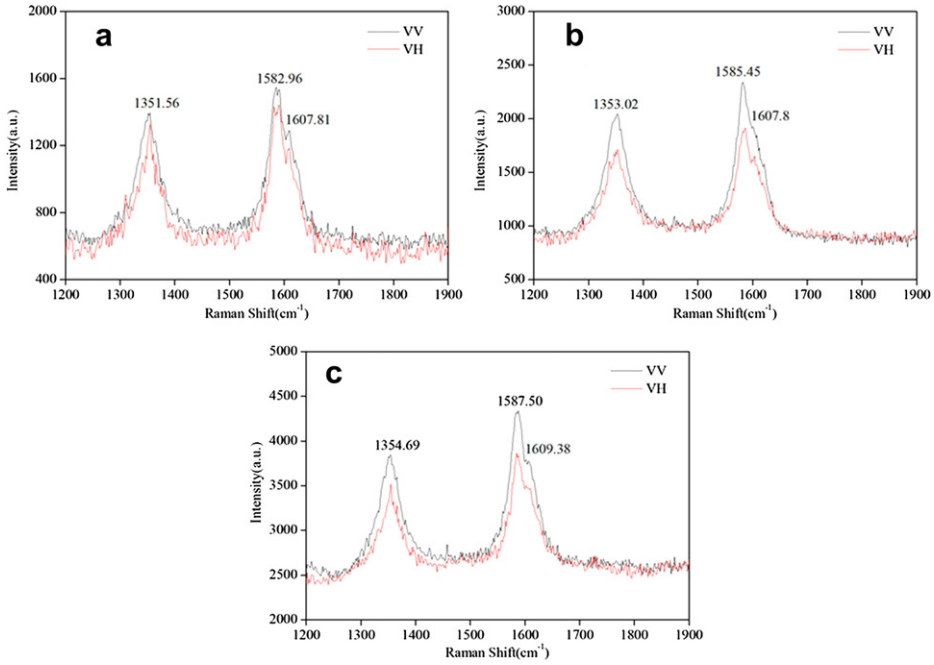

Fig. 5. Polarized Raman spectra of MWNTs-EP/PSF hybrid nanofibers with (a) 5 (b) 10, and (c)15 wt% MWNTs-EP.

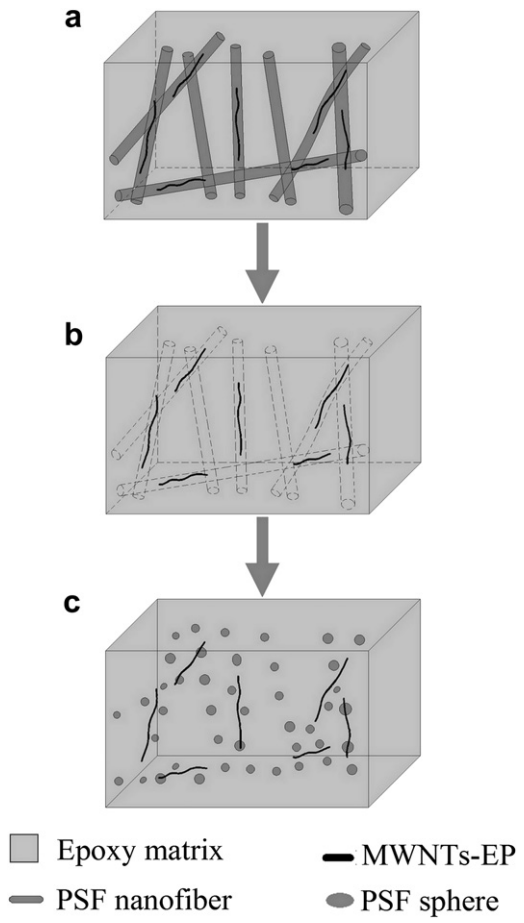

Fig. 6. Schematic representation of the dispersion and alignment states of MWNTs-EP during reaction-induced phase separation in RTEP. (a) Recombination of epoxy matrix and hybrid nanofibers, (b) Dissolution of PSF nanofibers into epoxy matrix, and (c) PSF spheres from the phase separation of nanofibers and fixation of MWNTs-EP in the phase structures.

depolarization factor *R*, the ratio of the peak intensities of the G band in the two polarization directions. The *R* values for hybrid nanofibers with 5, 10, and 15 wt % MWNTs-EP were 0.977, 1.070, and 1.152, respectively, which were greater than that of as-received MWNTs (ca. 0.81) [28]. The increase in *R* value can be ascribed to the better alignment of MWNTs-EP in the hybrid nanofibers with increasing MWNTs-EP loadings.

3.3. Prescribed morphology of hybrid nanofibers reinforced and toughened epoxy

The ex-situ dispersion and alignment of MWNTs-EP were obtained by fabricating MWNTs/PSF hybrid nanofibers through electrospinning, which was associated with the phase separation of MWNTs-EP/PSF hybrid nanofibers reinforced and toughened epoxy matrix (RTEP). Fig. 6 shows the schematic representation of the dispersion and alignment states of MWNTs-EP during reaction-induced phase separation in RTEP.

The epoxy matrix was compounded with MWNTs-EP/PSF hybrid nanofibers (a). During the curing process, PSF nanofibers were dissolved into epoxy matrix, whereas MWNTs-EP retained the original distribution as in hybrid nanofibers, as shown in (b).

With the curing reaction proceeding, the phase separation of hybrid nanofibers began to occur, and PSF spheres were generated due to phase separation of nanofibers, shown in (c). Herein, the distribution and alignment states between MWNTs-EP and PSF spheres were suggested. The first possible state was that the MWNTs-EP was enveloped by many PSF spheres, which was the most frequent. Another state was that MWNTs-EP might be pinned by one PSF sphere. In addition, the MWNTs-EP might also be bridged by some PSF spheres. However, whatever state the MWNTs-EP located among PSF spheres, the MWNTs-EP were almost dispersed and aligned along the original nanofiber direction, which was attributed to the dispersion and alignment of MWNTs-EP in hybrid nanofibers. The dispersion and alignment of MWNTs-EP and the generation of PSF spheres would result in the synergistic effects of hybrid nanofibers on reinforcing and toughening the epoxy matrix.

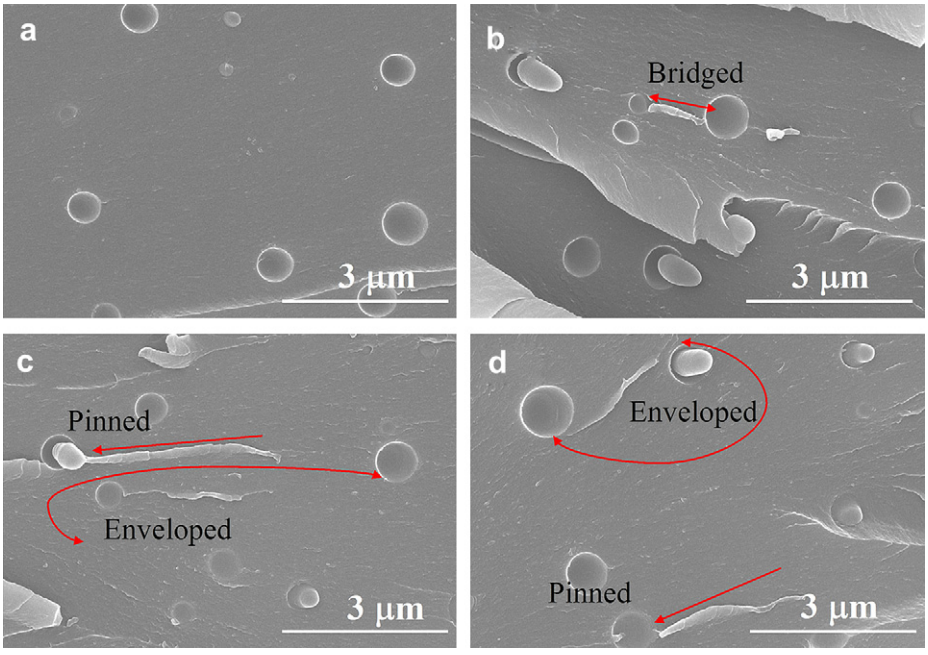

Fig. 7. SEM images of RTEP with (a) 0, (b) 0.1, (c) 0.2 and (d) 0.3 wt% MWNTs-EP.

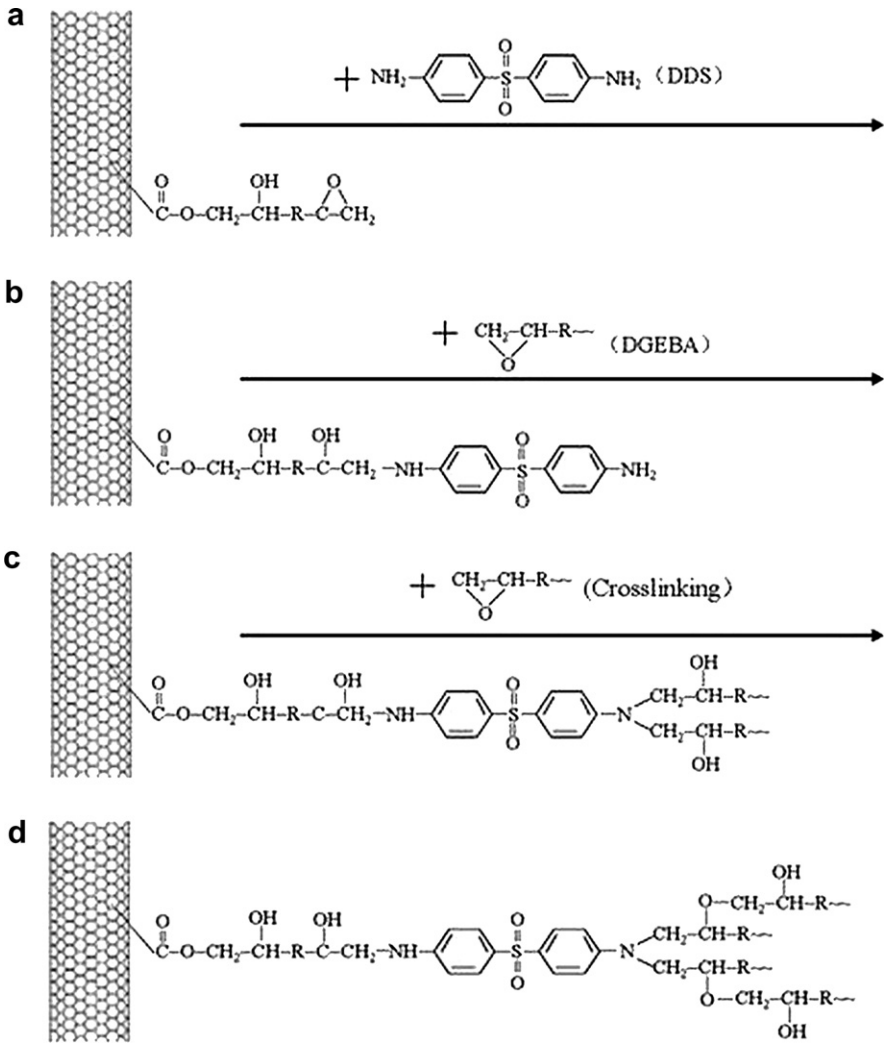

Fig. 8. Schematic of interface chemical reactions between MWNTs-EP and DGEBA.

According to the aforementioned schematic representation, the prescribed morphology of RTEP was confirmed. Fig. 7 shows the SEM images of RTEP with various MWNTs-EP loadings. The inhomogeneous phase separation occurred, and PSF spheres were aligned along the original nanofiber directions, which agreed with the results of our previous work [24]. As expected, MWNTs-EP were also dispersed and aligned along the line trace of PSF spheres. As discussed in the section above, MWNTs-EP were dispersed and aligned along the nanofiber axis. Therefore, MWNTs-EP were fixed along the nanofiber directions during reaction-induced phase separation of hybrid nanofibers. In addition, the distributed and oriented states between MWNTs-EP and PSF spheres were observed, which was consistent with the schematic representation in Fig. 6. MWNTs-EP were bridged by two PSF spheres in Fig. 7b, and MWNTs-EP, which possessed strong interfacial adhesion with epoxy matrix, were enveloped by some PSF spheres or pinned by one PSF sphere after phase separation in Fig. 7c. As shown in Fig. 7d, MWNTs-EP, which were embedded and held in epoxy matrix, were pinned by one PSF sphere or enveloped by some PSF spheres. However, regardless of the states between MWNTs-EP and PSF spheres, the alignment of PSF spheres and MWNTs-EP was beneficial to inhibiting the extension of cracks and achieving the efficient transfer of interfacial stress [29,30], which contributed to the synergistic effects of reinforcing of MWNTs-EP and toughening of PSF spheres.

3.4. Interface correlation between MWNTs-EP and epoxy matrix

Besides the dispersion and alignment of MWNTs-EP, the strong interfacial interaction between MWNTs-EP and epoxy matrix would be favorable to maximize the reinforcement of MWNTs [1,6].

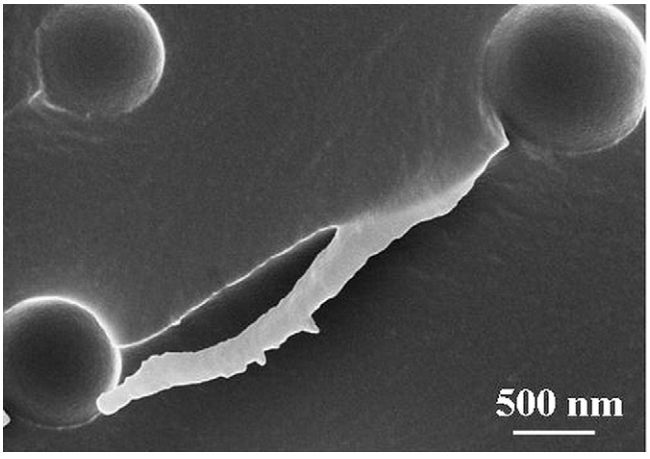

Fig. 9. SEM image of RTEP with 0.3 wt % MWNTs-EP.

Table 1
Tensile properties of MWNTs-EP/PSF hybrid nanofibers reinforced and toughened epoxy matrix (RTEP) with various MWNTs-EP loadings.

MWNTs-EP loading	Tensile strength (MPa)	Young's modulus (MPa)	Elongation at break (%)
0 wt %	59.9 ± 2.8	1782 ± 51	5.06 ± 0.4
0.1 wt %	64.9 ± 3.3	2062 ± 55	4.10 ± 0.4
0.2 wt %	70.8 ± 3.5	2078 ± 72	4.16 ± 0.3
0.3 wt %	76.0 ± 3.8	2118 ± 68	4.46 ± 0.4

From Fig. 7, the MWNTs-EP with high dispersion and alignment were observed to have stronger interactions with epoxy matrix, which was attributed to the increased polarity of MWNTs-EP by the functional groups and the possible interfacial reaction of epoxide groups with curing agent [7]. Fig. 8 shows the schematic of interface chemical reactions between MWNTs-EP and DGEBA. Due to the existence of DGEBA on the surface of MWNTs-EP, the epoxide ring was reacted with the primary amine of DDS and ring opening occurred, as shown in (a). Subsequently, the addition reaction of primary amine and epoxide groups of DGEBA continued, shown in (b). Finally, the further addition of amine to epoxide groups of epoxy matrix (c) would make MWNTs-EP become an integral part of crosslinking network structure (d) [3], which led to strong interfacial chemical interaction between MWNTs-EP and epoxy matrix. Therefore, MWNTs-EP could help the reinforced and toughened epoxy matrix bear larger external load and block the distortion.

Fig. 9 shows the SEM image of RTEP containing 0.3 wt % MWNTs-EP. The surfaces of MWNTs-EP were covered with thick-layer resin, which indicated the stronger interfacial interaction between MWNTs-EP and epoxy matrix. The MWNTs-EP were clearly "bridged" by the PSF spheres. The interface correlation between MWNTs-EP and epoxy matrix, and the distribution and alignment states of the MWNTs-EP in epoxy matrix would also be beneficial to realizing the synergistic effects of reinforcing and toughening the epoxy matrix.

3.5. Mechanical and thermal properties of reinforced and toughened epoxy matrix

Table 1 shows the tensile properties of MWNTs-EP/PSF hybrid nanofibers reinforced and toughened epoxy matrix (RTEP) with various MWNTs-EP loadings. The tensile strength of PSF nanofibers toughened epoxy matrix was 59.9 ± 5 MPa. However, the tensile strength of RTEP with 0.1, 0.2, and 0.3 wt % MWNTs-EP was increased by 8.3, 18.2, and 26.9%, respectively. The Young's modulus of RTEP with 0.3 wt % MWNTs-EP was 19% higher than that of PSF nanofibers toughened epoxy matrix. There was a moderate increase in both tensile strength and Young's modulus for RTEP with increasing MWNTs-EP loadings, which implied the reinforcing effect of MWNTs-EP and the effective load transfer resulted from the interfacial bonding between MWNTs-EP and epoxy matrix. Compared to PSF nanofibers toughened epoxy matrix, the elongation at break of RTEP showed a little decrease. However, the elongation at break of RTEP increased slightly with increasing MWNTs-EP loadings. The bridging crazes resulting from MWNTs-EP was favorable to the yield and slip of MWNTs-EP in epoxy matrix [31], which led to the increase of the elongation at break. The improvement of tensile properties reflected the synergistic effects of reinforcing and toughening resulting from MWNTs-EP with high strength and modulus and the PSF nanofibers with high toughness.

Fig. 10 shows the storage modulus (E') and tan δ spectra of RTEP with various MWNTs-EP loadings. The storage modulus of RTEP was higher than that of PSF nanofibers toughened epoxy matrix. With increasing the loading of MWNTs-EP, the storage modulus of RTEP increased gradually, which indicated that the stiffness of the composites was improved steadily [27]. The single peak in tan δ spectra demonstrated the good compatibility between epoxy matrix and PSF nanofibers. The glass transition temperatures (T_g) of RTEP with 0, 0.1, 0.2, and 0.3 wt % MWNTs-EP were 185.4, 188.1, 190.4, and 192.5 °C, respectively. The T_g of RTEP was increased with increasing MWNTs-EP loadings. This increase was due to the addition of MWNTs-EP, which also implied the reinforcing effect of MWNTs-EP.

The critical stress intensity factor (K_{IC}) was an important fracture toughness parameter, which described the stress state in the tip vicinity of a crack at fracture as functions of the specimen geometry, the crack geometry, and the applied load on the basis of linear elastic fracture mechanics [32]. Fig. 11 shows the K_{IC} of RTEP with various MWNTs-EP loadings.

The K_{IC} of PSF nanofibers toughened epoxy matrix was 3.11 MPa $m^{1/2}$. With increasing MWNTs-EP loadings, K_{IC} increased initially, and then decreased, which was similar to the results from Zhou [33]. The K_{IC} of RTEP with 0.1 wt % MWNTs-EP, was 45.8% higher than that of PSF nanofibers toughened epoxy matrix. Also, The K_{IC} of RTEP with 0.2 and 0.3 wt % MWNTs-EP were higher than that of PSF nanofibers toughened epoxy matrix, which implied the synergistic effects of reinforcing and toughening from MWNTs-EP and PSF nanofibers.

The toughening effect was dependent on the compatibility between epoxy matrix and PSF nanofibers, and also the formation of PSF spheres which resulted from phase separation of PSF nanofibers. Our previous works [23] have shown that the good compatibility and inhomogeneous phase separation resulted in the favorable toughening effects. The reinforcing effects depended on the interfacial interaction between MWNTs-EP and epoxy matrix, and the dispersion and alignment of MWNTs-EP in epoxy matrix. The dispersion and alignment of MWNTs-EP could avoid the localization of stress concentration, and the interfacial bonding

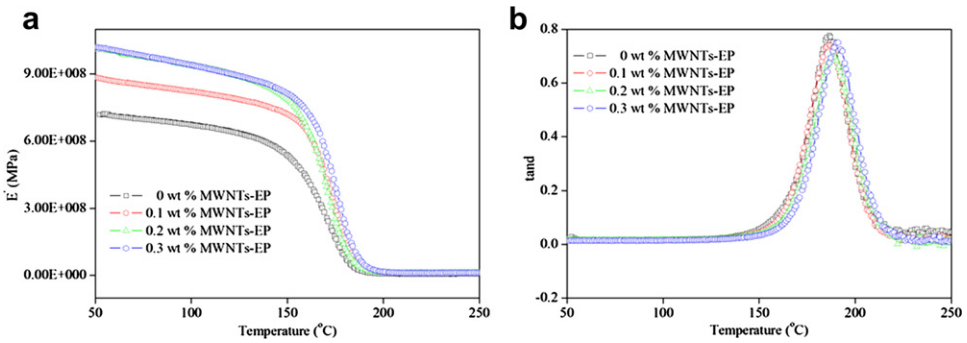

Fig. 10. (a) Storage modulus (E') and (b) tan δ spectra of RTEP with various MWNTs-EP loadings.

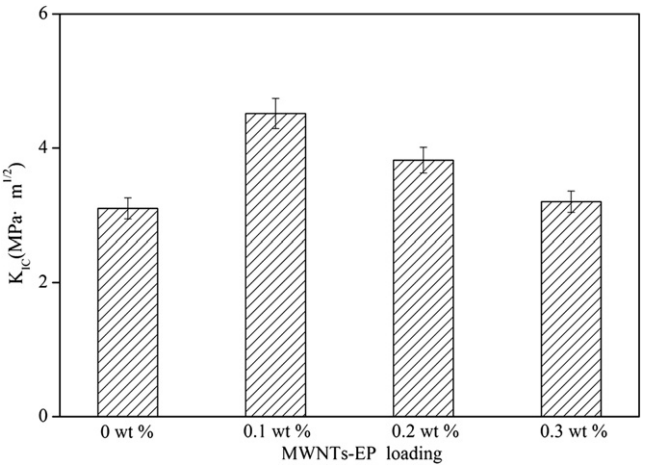

Fig. 11. K_{IC} of RTEP with various MWNTs-EP loadings.

between MWNTs-EP and epoxy matrix could achieve effective load transfer across the filler-matrix interface, which was demonstrated by the improvement of strength and modulus with increasing MWNTs-EP loadings. However, too strong interfacial adhesion between MWNTs-EP and matrix negatively affected the toughness by suppressing interfacial failure [7], which demonstrated by the decrease of K_{IC} with increasing MWNTs-EP loadings. Most importantly, the synergistic effects of reinforcing and toughening were obtained by the prescribed morphology and interface correlation during phase separation in RTEP.

4. Conclusion

The prescribed morphology and interfacial correlation of MWNTs-EP/PSF hybrid nanofibers reinforced and toughened epoxy matrix (RTEP) were obtained from ex-situ dispersion and alignment of functionalized MWNTs-EP through electrospinning. During the reaction-induced phase separation in RTEP, MWNTs-EP were enveloped, bridged or pinned by PSF spheres generated from the phase separation of hybrid nanofibers. The interfacial chemical interaction between MWNTs-EP and epoxy matrix was significantly improved by the reactive ability of epoxide groups on the surface of MWNTs-EP. The prescribed morphology and interfacial correlation resulted in the synchronous enhancement of strength, toughness and heat resistance of RTEP, which opened up the practical idea of preparing high performance interlaminar reinforced and toughened fiber/epoxy composites.

Acknowledgments

The authors would like to thank the National Natural Science Foundation of JiangSu Province (BK2011227) and the National Natural Science Foundation of China (50873010) for supporting this project.

References

[1] C.H. Tseng, C.C. Wang, C.Y. Chen, Chem. Mater. 19 (2007) 308.
[2] M. Moniruzzaman, K.I. Winey, Macromolecules 39 (2006) 5194.
[3] J. Zhu, H. Peng, F. Rodriguez-Macias, J.L. Margrave, V.N. Khabashesku, A.M. Imam, K. Lozano, E. Barrera, Adv. Funct. Mater. 14 (2004) 643.
[4] J. Shen, W. Huang, L. Wu, Y. Hu, M. Ye, Compos. Sci. Technol. 67 (2007) 3041.
[5] W. Jeong, M.R. Kessler, Chem. Mater. 20 (2008) 7060.
[6] J.N. Coleman, U. Khan, W.J. Blau, Y.K. Gunko, Carbon 44 (2006) 1624.
[7] F.H. Gojny, M.H.G. Wichmann, B. Fiedler, K. Schulte, Compos. Sci. Technol. 65 (2005) 2300.
[8] P.C. Ma, S.Y. Mo, B.Z. Tang, J.K. Kim, Carbon 48 (2010) 1824.
[9] C. Gao, C.D. Vo, Y.Z. Jin, W. Li, S.P. Armes, Macromolecules 38 (2005) 8634.
[10] J. Gao, B. Zhao, M.E. Itkis, E. Bekyarova, H. Hu, V. Kranak, A. Yu, R.C. Haddon, J. Am. Chem. Soc. 128 (2006) 7492.
[11] A. Eitan, K. Jiang, Chem. Mater. 15 (2003) 3198.
[12] W.S. Dale, S.J. Ryan, Macromolecules 40 (2007) 8501.
[13] R.A. Vaia, J.F. Maguire, Chem. Mater. 19 (2007) 2736.
[14] X.L. Xie, Y.W. Mai, X.P. Zhou, Mater. Sci. Eng. R 49 (2005) 89.
[15] A.M.K. Esawi, M.M. Farag, Mater. Design 28 (2007) 2394.
[16] N.R. Raravikar, L.S. Schadler, A. Vijayaraghavan, Y. Zhao, B. Wei, M. Pulickel Ajayan, Chem. Mater. 17 (2005) 974.
[17] W. Feng, X.D. Bai, Y.Q. Lian, J. Liang, X.G. Wang, K. Yoshino, Carbon 41 (2003) 1551.
[18] M.J. Casavant, D.A. Walters, J.J. Schmidt, R.E. Smalley, J. Appl. Phys. 93 (2003) 2153.
[19] Z.F. Ren, Z.P. Huang, D.Z. Wang, J.G. Wen, J.W. Xu, J.H. Wang, L.E. Calvet, J. Chen, J.F. Klemic, M.A. Reed, Appl. Phys. Lett. 75 (1999) 1086.
[20] H. Fong, W. Liu, C.S. Wang, R.A. Vaia, Polymer 43 (2002) 775.
[21] J. Ji, G. Sui, Y. Yu, Y. Liu, Y. Lin, Z. Du, S. Ryu, X. Yang, J. Phys. Chem. C 113 (2009) 4779.
[22] D. Yael, S. Wael, L.K. Rafail, C. Yachin, L.Y. Alexander, Z. Eyal, Langmuir 19 (2003) 7012.
[23] G. Li, P. Li, C. Zhang, Y. Yu, H. Liu, S. Zhang, X. Jia, X. Yang, Z. Xue, S. Ryu, Compos. Sci. Technol. 68 (2008) 987.
[24] G. Li, Z. Huang, C. Xin, P. Li, X. Jia, B. Wang, Y. He, S. Ryu, X. Yang, Mater. Chem. Phys. 118 (2009) 398.
[25] H. Fong, I. Chun, D.H. Reneker, Polymer 40 (1999) 4585.
[26] S.F. Fennessey, R.J. Farris, Polymer 45 (2004) 4217.
[27] J. Yang, T. Xu, A. Lu, Q. Zhang, H. Tan, Q. Fu, Compos. Sci. Technol. 69 (2009) 147.
[28] C. Gao, Y.Z. Jin, H. Kong, R.L.D. Whitby, S.F.A. Acquah, G.Y. Chen, H.H. Qian, A. Hartschuh, S.R.P. Silva, S. Henley, P. Fearon, H.W. Kroto, D.R.M. Walton, J. Phys. Chem. B 109 (2005) 119.
[29] Y.S. Song, J.R. Youn, Carbon 43 (2005) 1378.
[30] Y. Ye, H. Chen, J. Wu, L. Ye, Polymer 48 (2007) 6426.
[31] L. Jin, C. Bower, O. Zhou, Appl. Phys. Lett. 73 (1998) 1197.
[32] S.J. Park, M.H. Kim, J.R. Lee, S. Choi, J. Colloid, Interf. Sci. 228 (2000) 287.
[33] Y. Zhou, F. Pervin, L. Lewis, S. Jeelani, Mater. Sci. Eng. A 475 (2008) 157.